

X-Ray Reflectivity and Scanning-Tunneling-Microscope Study of Kinetic Roughening of Sputter-Deposited Gold Films during Growth

H. You, R. P. Chiarello,^(a) H. K. Kim,^(b) and K. G. Vandervoort

Materials Science Division, Argonne National Laboratory, Argonne, Illinois 60439

(Received 16 November 1992)

An *in situ* x-ray reflectivity study of the dynamic evolution of a growing interface was carried out for gold sputter-deposited onto a polished silicon substrate. X-ray reflectivity data were recorded during growth for thicknesses of the gold film ranging from 50 to 3500 Å. A progressive kinetic roughening of the gold-vacuum interface was observed and the time-dependent interfacial width exhibits a power-law behavior. Aided by scanning-tunneling-microscopy measurements the scaling exponents were determined and compared with theoretical studies.

PACS numbers: 61.10.-i, 68.45.Da, 82.65.Dp

Nonequilibrium growth of thin films by deposition from the vapor phase is of considerable practical and scientific interest. In particular, recent computational studies of diffusion-limited aggregation and the Eden process made the observation that growth occurs mainly at the *active zone* [1] with possible scaling behavior [2]. This observation has stimulated numerous analytical and computational studies on different models and dimensions. The central idea is the scaling behavior of the interfacial width W [2],

$$W(L, t) \sim L^\chi f(t/L^{\chi/\beta}) \quad (1)$$

with a finite-size scaling exponent, χ , and a dynamic scaling exponent, χ/β , for a system of size L at time t . Following the initial observations of this scaling behavior, Kardar, Parisi, and Zhang [3] proposed a simple nonlinear Langevin equation (KPZ equation) to analytically describe the nature of the growing interface. From this equation they found exponents for 1+1 dimensions consistent with those found in several computational studies and they speculated about possible universal behavior. For higher dimensions, the situation is less definite and the exponents found in various studies [4-6] are not in good agreement.

The purpose of this study was to experimentally check the scaling behavior and to determine the exponents for nonequilibrium growth during sputter deposition. Most recent computational studies have used ballistic deposition models because of their close resemblance to real experimental deposition conditions [2, 6]. The sputtering technique was chosen in our investigation because of its flexibility in changing the deposition rate and the deposited particle momenta. Also x-ray techniques are unique for the sputtering environment because Ar pressure in a sputtering chamber is generally too high for *in situ* examination with electron-based techniques [7].

X-ray reflectivity (XR) and scanning tunneling microscopy (STM) were used to characterize the growing interface. Specular XR scans were recorded during growth to extract the time evolution of the interfacial width. From the STM study, topographic images were recorded

and these images were used to characterize the interface as a complement to the XR measurements.

The x-ray measurements were performed at beamline X22B, at the National Synchrotron Light Source in a horizontal scattering geometry with a longitudinal instrumental resolution [8] of $\sim 1 \times 10^{-3} \text{ \AA}^{-1}$. Six series of specular XR scans were made during sputter deposition of gold particles at three substrate temperatures (220, 300, and 350 K) and at two Ar pressures (1 and 10 mTorr). The Ar pressures were chosen so that the gold particles sputtered from the target *either* thermalized completely via collisions before they hit the surface (at 10 mTorr) *or* suffered nearly no collision and arrived at the surface with large momenta following straight trajectories (at 1 mTorr). The specular and off-specular reflectivity data and STM images [9, 10] consistently suggest that the high-pressure films were rough locally but smooth globally and *incoherent averaging* [11, 12] was not needed in data analysis while the opposite was true for the low-pressure films. In this Letter only a brief description of experiments and the high-pressure data taken at 220 and 300 K will be presented. The experimental details and remaining data will be presented in a later publication [9].

A sputtering chamber described previously [7] equipped with a faced magnetron sputter system [7] was modified by adding a liquid-nitrogen-cooled sample stage for these experiments. The substrates were commercially prepared polished silicon (111) single crystals with surface areas of $\sim 1 \times 1 \text{ cm}^2$ and measured root-mean-square roughnesses of $\sim 3 \text{ \AA}$. They were cleaned by a wet process and were then baked inside the chamber until no surface contamination was detected in XR scans.

The deposition rate was $\sim 0.5 \text{ \AA/sec}$ and we will refer to the deposition time t in units of Å (2 sec) throughout this paper. At the end of each series of measurements the samples were brought out to the air at room temperature for further examinations. The further x-ray examination included off-specular XR measurements and determination of preferred orientations of the film [9]. In addition, STM images of the gold surface were obtained using a

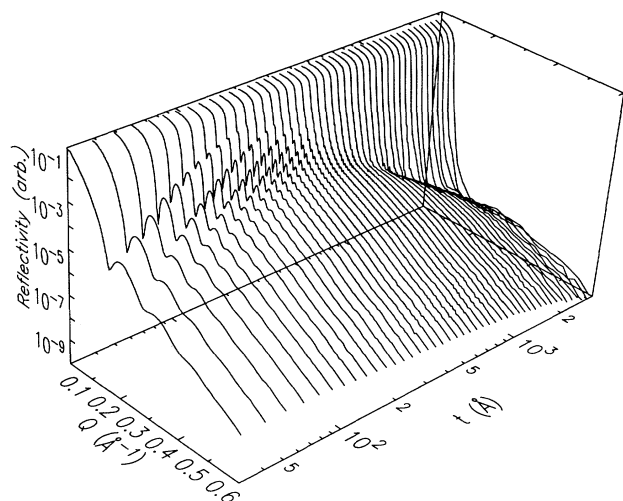


FIG. 1. Time evolution of specular x-ray reflectivity measured during the deposition at 10 mTorr Ar pressure and 220 K. The time axis is shown in units of Å for a deposition rate of 0.5 Å per second.

STM operating at 100 mV bias voltage and 100 pA tunneling current.

A series of successive specular XR scans measured at 220 K and 10 mTorr and corrected for background [9] are shown in Fig. 1. The oscillations in the XR scans are due to interference between the reflection amplitudes from the gold-vacuum and gold-substrate interfaces. The oscillation period is inversely proportional to the gold thickness and the amplitude contains information on the interfacial widths of the two interfaces. For thick films the interference fringes disappear due to finite instrumental resolution and due to interface roughness; the XR then can be approximated by summing the reflected intensities from each interface. All the XR scans in this series were well described by a single reflectivity equation and derivation of the equation is discussed below.

An interface in d_s+1 dimensions can be described by a single valued function $h(\mathbf{r}, t)$ when the structure is sufficiently compact and overhangs can be ignored [3]. Here \mathbf{r} is a d_s -dimensional vector and t is equivalent to the +1-dimensional axis scaled by a constant growth rate. Then we can define an equal time *height difference distribution function*, $G(r, t)$ [13], which depends on the distance r between two points and on time t , as

$$G(\mathbf{r}, t) = \left\langle |h(\mathbf{r} + \mathbf{r}_1, t) - h(\mathbf{r}_1, t)|^2 \right\rangle_{\mathbf{r}_1}, \quad (2)$$

where it is assumed that the interface is isotropic within the surface dimension d_s . Then for 2+1 dimensions the square of the interfacial width, $W(L, t)$, can be obtained by averaging over an area πL^2 ,

$$W^2(L, t) = \frac{2}{L^2} \int_0^L G(r, t) r dr. \quad (3)$$

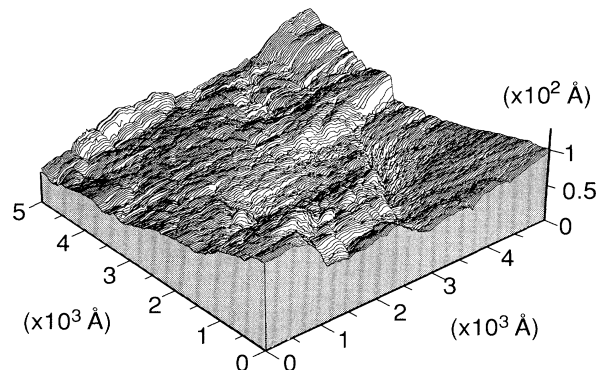


FIG. 2. STM topograph of the 3500 Å thick sample grown at 10 mTorr Ar pressure and 220 K.

As long as the scaling behavior proposed in Eq. (1) is assumed, the asymptotic behavior of $G(r, t)$ can be found from Eq. (3) and the asymptotic behavior of the scaling function $f(x)$ [see Eq. (4b) of Ref. [14]] without detailed knowledge of the interface morphology $h(\mathbf{r}, t)$ [4],

$$G(r, t) \sim \begin{cases} r^{2\chi} & \text{for } r^\chi \ll t^\beta, \\ t^{2\beta} & \text{for } t^\beta \ll r^\chi. \end{cases} \quad (4a)$$

$$(4b)$$

For a fixed time, t , $G(r, t)$ grows as $r^{2\chi}$ for small r and reaches a saturation value of $\sim t^{2\beta}$ for large r . From Eq. (3) the saturation value is $W^2(t) \equiv W^2(\infty, t)$. Consequently $W^2(t)$ has a power-law dependence on t with an exponent 2β .

The height difference distribution function, $G(r, t = 3500 \text{ Å})$, was calculated from the STM image shown in Fig. 2. A 200×200 grid was used for the calculations and $G(r, t = 3500 \text{ Å})$ is shown in Fig. 3(a) as the solid line. Despite some uncertainty in height calibration of the STM [15], $G(r, t = 3500 \text{ Å})$ shows the smooth increase for small distances ($r < 2000 \text{ Å}$) and saturates to a constant value at large distances ($r > 5000 \text{ Å}$). Because of finite sampling and noise in measurements [15], we do not prove the finite-size scaling behavior. Instead, a fit to the data ($r < 2000 \text{ Å}$) was made with an assumption of power-law behavior and the dashed line shows the best fit with $\chi=0.42(3)$.

The XR was analyzed using a specular reflectivity equation for two interfaces (gold vacuum and gold substrate),

$$I = A \left| V_1 P(Q_1, W) + V_2 e^{-\frac{1}{2} Q_2^2 \sigma^2 + i Q_{Au} t} \right|^2, \quad (5)$$

similar to that of Ref. [11]. V 's are Fresnel amplitudes for ideally sharp interfaces, $Q_1 = \sqrt{Q Q_{Au}}$ and $Q_2 = \sqrt{Q_{Si} Q_{Au}}$ [16] with $Q_{Au, Si} = \sqrt{Q^2 - K^2(1 - \epsilon_{Au, Si})}$. Complex dielectric constants, ϵ_{Au} and ϵ_{Si} , were used to account for absorption effects. The roughness of the substrate, $\sigma = 3 \text{ Å}$, and the overall factor, A , were predetermined. Addition of multiple scattering marginally

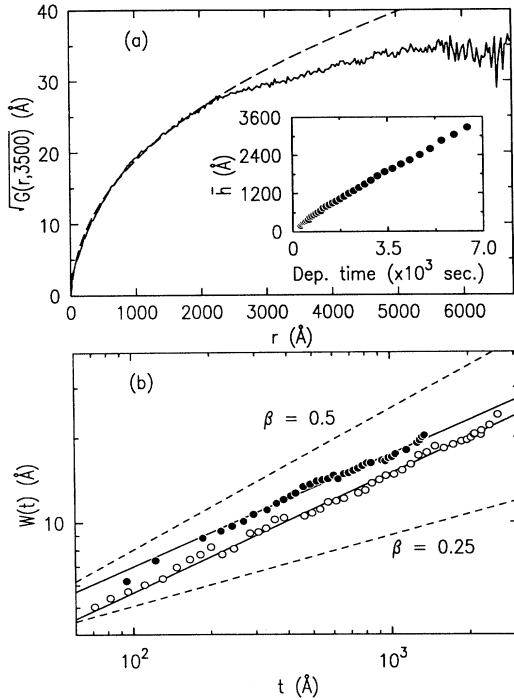


FIG. 3. (a) $\sqrt{G(r, t)}$ at $t = 3500 \text{ \AA}$ (solid line) calculated from the STM image in Fig. 2 using a power-law fit (dashed line). The thickness of the film $\langle h \rangle$ vs the deposition time in seconds is shown in the inset. (b) The surface widths of gold films grown at 220 K (open circles) and 300 K (filled circles). The widths were measured from the specular x-ray reflectivity scans. The solid lines are the power-law fits to the data and two dashed lines ($\beta=0.25$ and 0.5) are shown for reference.

improved fits but had negligible effect on the value of W . The Fourier transformation of the gold-vacuum interface profile is described by $P(Q, W) = \frac{2}{D^2} \int_0^D e^{-Q^2 G(r, t)/2} r dr$ where Q is the perpendicular momentum transfer and D^2 is the x-ray coherence area [16]. Since the analytic form of $G(r, t)$ is not known, we made an approximation for the analysis of the specular XR data that $G(r, t)$ changes from Eq. (4a) to Eq. (4b) at $r^x = t^\beta$. Then,

$$P(Q, W) = \frac{\{W(t)\}^{2/x}}{D^2} \left[\frac{1}{\chi y^{2/x}} \gamma \left(\frac{1}{\chi}, y^2 \right) \right] + \left\{ 1 - \frac{\{W(t)\}^{2/x}}{D^2} \right\} e^{-y^2}, \quad (6)$$

where $y = \sqrt{\frac{1}{2} Q^2 W^2(t)}$. The prefactor of the first term is the fraction of the x-ray coherence area where $G(r, t)$ is approximated to have a power-law dependence on r . The prefactor of the second term is the fractional area where $G(r, t)$ is approximated to be constant. The first term is required by the XR data. Figure 4 shows the specular XR data for the 3500 \AA thick film. The fit with a simple Gaussian distribution is shown as the dashed

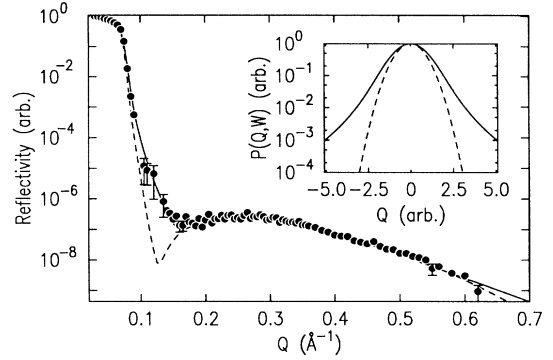


FIG. 4. The specular x-ray reflectivity scan for a thick film (3500 \AA thick) grown at 10 mTorr Ar pressure and 300 K. The solid and dashed lines are the fits to the data with the two different forms of $P(Q, W)$ shown in the inset.

line and the fit with Eq. (6) is shown by the solid line. The measured instrumental resolution sets $D = 5000 \text{ \AA}$ [9] and the analysis of the STM data sets $\chi = 0.4$. In the inset to Fig. 4 the Gaussian function and the factor in the square brackets of the first term are compared on a logarithmic scale.

A fit to the data to find the deposition rate was made with two parameters, the film thickness $\langle h \rangle$ and the interface width W [9]. $\langle h \rangle$ is plotted against the deposition time in the inset to Fig. 3(a). The deposition rate determined by a linear fit to $\langle h \rangle$ is $0.51(2) \text{ \AA/sec}$. The fit was then repeated for only one parameter, W , by setting the deposition rate to 0.51 \AA/sec . In Fig. 3(b) the time evolution of the interface width $W(t)$ for the 220 K (open circles) and 300 K (filled circles) XR data sets are shown in a log-log plot. The surface width exhibits a power-law time-dependent behavior consistent with the predicted scaling behavior over nearly 2 orders of magnitude in time. The exponent β was found by power-law fits to be $0.40(2)$ for the 300 K data and $0.42(2)$ for the 220 K data.

Now let us compare our results with recent theoretical and computational investigations on growing interfaces. Many of the investigations are based on the KPZ equation [3],

$$\frac{\partial h}{\partial t} = \nu \nabla^2 h + \frac{\lambda}{2} (\nabla h)^2 + \eta(\mathbf{r}, t), \quad (7)$$

where ν is the surface tension, λ is the coefficient of the lowest order nonlinear term, and η is a Gaussian random variable. For $\nu = \lambda = 0$, the KPZ equation is a trivial case of uncorrelated random deposition where β is the only relevant exponent and is equal to 0.5 for any spatial dimension [14]. Without the nonlinear term, i.e., $\lambda = 0$, the interfacial width should show a logarithmic time dependence [17]. For $\nu, \lambda \neq 0$ various computational studies on (2+1)-dimensional systems have reported that β is single valued in a strong coupling limit [4, 18], has a crossover from algebraic to power-law behavior in the

presence of a nonlocal field [5], and shows a dynamic phase transition depending on the relative strength of ν and λ [19].

Our experimental results indicate that (i) there is no apparent phase transition or crossover up to 3500 Å, (ii) the exponent χ and the functional form of $G(r, t)$ appear consistent, within our experimental uncertainty, with the results by Kim and Kosterlitz [4] and of Amar and Family [20], and (iii) our value for the exponent β is substantially larger than that predicted by most studies for 2+1 dimensions based on the KPZ equation.

The comparison of our results to studies based on the KPZ equation indicates that the description of experimental growth systems such as sputter deposition may require additional mechanisms beyond the KPZ equation. A recent renormalization analysis [21] included surface diffusion and explored the phase diagram which includes the KPZ phase. This study found significantly different values for the exponents from those based on the KPZ equation in other parts of the phase diagram. In our low pressure deposition measurements, where surface diffusion is expected to be significantly larger than in our high-pressure data, finite length-scale fluctuations were found in both the off-specular XR and the STM data [9]. These fluctuations appear consistent with the phase in the renormalization analysis which has a finite-wave-vector instability [21]. Therefore it is reasonable to speculate that a complete exploration of the phase diagram may lead to a region yielding exponents similar to our observed values. In a recent experimental study of a (1+1)-dimensional system [22] it was also found that the value of χ is consistent with the prediction based on the KPZ equation while the value of β is substantially larger.

In conclusion, we observed the time-dependent power-law behavior of the interfacial width of a growing interface in 2+1 dimensions and estimated the exponents χ and β from XR and STM data.

We thank Professor S. G. J. Mochrie and Professor L. B. Sorensen for helpful comments. We also thank J. Q. Zheng, T. Roberts, S. Williams, R.T. Kampwirth, D. Miller, K. E. Gray, and J. B. Ketterson for helping us in the early stages of this work. This work was supported by DOE under Contract No. W-31-109-Eng-38 (H.Y., R.P.C., H.K.K.) and the NSF Office of Science and Technology Centers, Science and Technology Center for Superconductivity, under Contract No. STC-8809854 (K.G.V.). One of us (H.K.K.) was also supported by Korean Science Foundation and RCDAMP.

- (a) New address: Chemical Technology Division, Argonne National Laboratory, Argonne, IL 60439.
 (b) On leave from Pusan National University, Department of Physics, Pusan, Korea.
- [1] M. Plischke and Z. Racz, *Phys. Rev. Lett.* **53**, 415 (1984).
 - [2] F. Family and T. Vicsek, *J. Phys. A* **18**, L75 (1985).
 - [3] M. Kardar, G. Parisi, and Y. Zhang, *Phys. Rev. Lett.* **56**, 889 (1986).
 - [4] J.M. Kim and J.M. Kosterlitz, *Phys. Rev. Lett.* **62**, 2289 (1989); J.M. Kim, J.M. Kosterlitz, and T. Ala-Nissila, *J. Phys. A* **24**, 5569 (1991).
 - [5] J. Krug and P. Meakin, *Phys. Rev. Lett.* **66**, 703 (1991).
 - [6] R.P.U. Karunasiri, R. Bruinsma, and J. Rudnick, *Phys. Rev. Lett.* **62**, 788 (1989).
 - [7] D.J. Miller, R.P. Chiarello, H.K. Kim, T. Roberts, H. You, R.T. Kampwirth, K.E. Gray, J.Q. Zheng, S. Williams, J.B. Ketterson, and R.P.H. Chang, *Appl. Phys. Lett.* **59**, 3174 (1991).
 - [8] The coherence lengths of longitudinal and transverse directions are 6800 and 2500 Å, respectively. We assume an isotropic coherence length of 5000 Å in our data analysis.
 - [9] R.P. Chiarello, H. You, H.K. Kim, and K.G. Vandervoort (to be published).
 - [10] National Synchrotron Light Source Annual Report, 1991 (unpublished), Vol. II, p. 253.
 - [11] H. You, C.A. Melendres, Z. Nagy, V.A. Maroni, W. Yun, and R.M. Yonco, *Phys. Rev. B* **45**, 11 288 (1992).
 - [12] S. Garoff, E.B. Sirota, S.K. Sinha, and H.B. Stanley, *J. Chem. Phys.* **90**, 7505 (1989).
 - [13] Its relation to a height-height correlation function $C(\mathbf{r})$ is $G(\mathbf{r}) = W^2(t) [1 - C(\mathbf{r})]$; M.V. Berry, *Philos. Trans. Roy. Soc. A* **273**, 611 (1973).
 - [14] K.G. Vandervoort, R.K. Zasadzinski, G.G. Galicia, and G.W. Crabtree, *Rev. Sci. Instrum.* (to be published).
 - [15] S.K. Sinha, E.B. Sirota, S. Garoff, and H.B. Stanley, *Phys. Rev. B* **38**, 2297 (1988).
 - [16] F. Family, *Physica (Amsterdam)* **168A**, 561 (1990).
 - [17] S.F. Edwards and D.R. Wilkinson, *Proc. R. Soc. London A* **381**, 17 (1982).
 - [18] D.E. Wolf and J. Kertesz, *Europhys. Lett.* **4**, 651 (1987).
 - [19] H. Yan, D. Kessler, and L.M. Sander, *Phys. Rev. Lett.* **64**, 926 (1990); in our study only β (not χ) was continuously measured and no abrupt change was found.
 - [20] J.G. Amar and F. Family, *Phys. Rev. Lett.* **64**, 543 (1990).
 - [21] L. Golubovic and R. Bruinsma, *Phys. Rev. Lett.* **66**, 321 (1991).
 - [22] G.L.M.K.S. Kahanda, X. Zou, R. Farrell, and P. Wong, *Phys. Rev. Lett.* **68**, 3741 (1992); another study suggesting a larger β in 2+1 dimensions is J. Chevrier, V. Le Thanh, R. Buys, and J. Derrien, *Europhys. Lett.* **16**, 737 (1991).